Magnetic properties and ^{155}Gd Mössbauer spectroscopy of the icosahedral quasicrystal Ag$_{50}$In$_{36}$Gd$_{14}$

Magnetic properties and ^{155}Gd Mössbauer spectroscopy of the icosahedral quasicrystal Ag$_{50}$In$_{36}$Gd$_{14}$

Zbigniew M Stadnik[1]**, Khalid Al-Qadi and Pu Wang**

Department of Physics, University of Ottawa, Ottawa, ON, K1N 6N5, Canada

E-mail: stadnik@uottawa.ca

Abstract

The results of x-ray diffraction, magnetic susceptibility, and ^{155}Gd Mössbauer spectroscopy studies of the recently discovered icosahedral quasicrystal Ag$_{50}$In$_{36}$Gd$_{14}$ are reported. The studied quasicrystal has a simple six-dimensional Bravais lattice with the six-dimensional hypercubic lattice constant of 7.805(2) Å. The observed broadening of the diffraction Bragg peaks reflects the presence of the topological/chemical disorder. The temperature dependence of the magnetic susceptibility follows the Curie–Weiss law with an effective magnetic moment of 8.15(1) μ_B per Gd atom and the paramagnetic Curie temperature of $-37.1(2)$ K. The studied quasicrystal is a spin glass with a freezing temperature of 4.25(5) K. The presence of a distribution of the electric quadrupole splitting in the Mössbauer spectra indicates the existence of a multiplicity of Gd sites. The values of the principal component of the electric field gradient tensor and the asymmetry parameter at these sites are, respectively, $-4.91(10) \times 10^{21}$ V cm^{-2} and $\eta = 1.00(20)$. The Debye temperature of Ag$_{50}$In$_{36}$Gd$_{14}$ is 199(2) K. The hyperfine magnetic field sets in at a temperature higher than the freezing temperature.

(Some figures in this article are in colour only in the electronic version)

1. Introduction

Solids are traditionally divided into two groups: crystalline and amorphous. The dramatic discovery of an icosahedral (i) Al–Mn alloy by Shechtman *et al* [1] extended this dichotomous division by introducing the notion of quasicrystals (QCs). These are materials that possess a new type of long-range translational order, *quasiperiodicity*, and a noncrystallographic orientational order associated with the classically forbidden fivefold, eightfold, tenfold, and

---

[1] Author to whom any correspondence should be addressed.

twelvefold symmetry axes [2]. A main problem in condensed matter physics is determining whether quasiperiodicity leads to physical properties which are significantly different from those of crystalline and amorphous materials of the same/similar compositions.

One of the central questions in the physics of QCs is that of the possibility of the existence of long-range magnetic order in these alloys. Initial intuition suggests that quasiperiodicity necessarily leads to geometrical frustration and is therefore incompatible with long-range magnetic order. However, various theoretical models dealing with magnetism in QCs indicate the possibility of existence of long-range magnetic order in QCs. There are geometrical models [3] and physical models, such as the Ising model [4], the XY model [5], the Heisenberg model [6], and the Hubbard model [7].

On the experimental side, all known QCs are either diamagnets, paramagnets or spin glasses [8]. The recent claim [9] of the existence of long-range magnetic order in i R–Mg–Zn (R = rare earth) QCs was shown [10] to result from the presence of magnetic impurities in the studied samples. Recent extensive neutron diffraction studies [11] of i R–Mg–Zn and i R–Mg–Cd QCs, which are of very high structural quality and which can be produced in a single-grain form, revealed the presence of short-range spin correlations at low temperatures and the absence of long-range magnetic order; these QCs are spin glasses.

Recently, new metastable i QCs were discovered in the $Ag_{50}In_{36}R_{14}$ system [12]. These QCs are formed by replacing all of Cd in the binary i $YbCd_{5.7}$ QC [13] with Ag and In, and Yb with other R elements. It is thus expected that the crystal structure of the i $Ag_{50}In_{36}R_{14}$ QCs must be similar to that of the i $YbCd_{5.7}$ QC. Very recently, the crystal structure of the i $YbCd_{5.7}$ QC has been solved [14]. It is based on three building units (rhombic triacontahedra linked with acute and obtuse rhombohedra) arranged quasiperiodically with unique atomic decorations. One would expect that R atoms are located at the Yb sites (on the vertices of the icosahedron and inside the acute rhombohedron) and the Ag and In atoms are distributed among the Cd sites. The new i $Ag_{50}In_{36}R_{14}$ QCs are expected to posses well localized and sizeable 4f magnetic moments on the R elements and perhaps exhibit long-range magnetic order. In this paper, we report on structural, magnetic, and ^{155}Gd Mössbauer spectroscopy studies of the i alloy $Ag_{50}In_{36}Gd_{14}$.

2. Experimental procedure

An ingot of nominal composition $Ag_{50}In_{36}Gd_{14}$ was prepared by melting constituent elements in an induction furnace on water-cooled Cu boat under an Ar atmosphere. Purities of the starting elements were 99.999%, 99.999%, and 99.998% for Ag, In, and Gd, respectively. The melting was repeated four times, in each case after turning the ingot. The total weight loss after the melting was 1.5%. The ingot was then melt spun in an Ar atmosphere by ejecting molten alloy through a 0.7 mm orifice in a quartz tube onto a surface of a copper wheel rotating with a tangential velocity of 47 m s^{-1}. The resulting ribbons were about 1.0 cm long and 20 μm thick.

X-ray diffraction (XRD) measurements were performed at 298 K in Bragg–Brentano geometry on a PANanalytical X'Pert scanning diffractometer using Cu Kα radiation. The Kβ line was eliminated by using a Kevex PSi2 Peltier-cooled solid-state Si detector. To allow for the possible instrumental aberration and specimen displacement, corrections were made to the 2θ angles using a fourth-order polynomial calibration curve [15] obtained from the scan of the specimen mixed with 10 wt% of a Si standard [16].

The magnetic susceptibility was measured with a Quantum Design superconducting quantum interference device magnetometer at various fields in the temperature range 2.0–300 K.

The ^{155}Gd Mössbauer spectroscopy measurements in the temperature range 1.5–10.4 K were conducted using a standard Mössbauer spectrometer operating in a sine mode and a source of ^{155}Eu(SmPd$_3$). The source was kept at the same temperature as that of the absorber. The spectrometer was calibrated with a Michelson interferometer [17], and the spectra were folded. The Mössbauer absorber was made of pulverized material pressed into a pellet which was then put into an Al disc container of thickness of 0.008 mm to ensure a uniform temperature over the whole sample. The surface density of the Mössbauer absorber of the i Ag$_{50}$In$_{36}$Gd$_{14}$ alloy was 304 mg cm^{-2}. The 86.5 keV γ-rays were detected with a 2.5 cm NaI(Tl) scintillation detector covered with a 0.6 mm Pb plate to cut off the 105.3 keV γ-rays emitted from the source.

The Mössbauer spectra were analysed by means of a least-squares fitting procedure which entailed calculations of the positions and relative intensities of the absorption lines by numerical diagonalization of the full hyperfine interaction Hamiltonian [18]. The following hyperfine parameters are obtained from the fits: the hyperfine magnetic field at a nuclear site, H_{hf}, the z-component of the electric field gradient (EFG) tensor, V_{zz}, the asymmetry parameter, η, defined as $\eta = |(V_{xx} - V_{yy})/V_{zz}|$ (if the principal axes are chosen such that $|V_{xx}| < |V_{yy}| < |V_{zz}|$, then $0 \leqslant \eta \leqslant 1$), the angle between the direction of H_{hf} and the V_{zz}-axis, θ, and the angle between the V_{xx}-axis and the projection of H_{hf} onto the xy-plane, ϕ. During the fitting procedure, the g-factor and the quadrupole moment ratios for ^{155}Gd ($I_g = 3/2$, $I_{ex} = 5/2$) were constrained to, respectively, $g_{ex}/g_g = 1.235$ and $Q_{ex}/Q_g = 0.087$ [19]. The interference ξ-factor for the E1 transition of 86.5 keV in ^{155}Gd was fixed to the value of 0.0520, which was derived from the fit of the ^{155}Gd Mössbauer spectrum of GdFe$_2$ at 4.2 K [20].

The resonance line shape of the Mössbauer spectra was described by a transmission integral formula [21]. In addition to the hyperfine parameters, only the absorber Debye–Waller factor f_a and the absorber linewidth Γ_a were fitted as independent parameters. The source linewidth $\Gamma_s = 0.334$ mm s^{-1} and the background-corrected Debye–Waller factor of the source f_s^* [22], which were derived from the fit of the ^{151}Gd Mössbauer spectrum of GdFe$_2$ at 4.2 K [20], were used. The ^{155}Eu(SmPd$_3$) source at 1.5 K emits a broadened emission line; from the fit of the ^{151}Gd Mössbauer spectrum of GdFe$_2$ at 1.5 K we found that $\Gamma_s = 0.708$ mm s^{-1} [20].

3. Results and discussion

3.1. Structural characterization

The XRD pattern of the studied sample measured in the 2θ range 5°–100° (figure 1) shows the presence of 19 i Bragg peaks, the weaker of which were not observed earlier [12] in the patterns obtained with a scintillation/proportional counter. Four weak Bragg peaks due to an unidentified second phase are also observed (figure 1). The positions of all the detected i Bragg peaks corresponding to Cu Kα_1 radiation (the value of its wavelength λ is 1.540 5981 Å [22]) in terms of the angle $2\theta_1$ and the corresponding wavenumber $Q_{exp} = 4\pi \sin\theta_1/\lambda$, as well as their relative intensities and full widths at half maximum Γ_Q, were determined from the profile fitting using the procedure described by Schreiner and Jenkins [23]. These parameters corresponding to 19 detected i peaks, whose positions are indicated by vertical lines in figure 1, are presented in table 1. This table also contains the theoretical positions Q_{cal} which were calculated by taking the position of the second most intense i peak as the reference. Since there are several schemes employed to index the i peaks, we present in table 1 the indices that correspond to the most frequently used schemes [24–26].

There is a good agreement between the observed Q_{exp} and the theoretical Q_{cal} positions of the i Bragg peaks (figure 1 and table 1). The absence of Bragg peaks that correspond
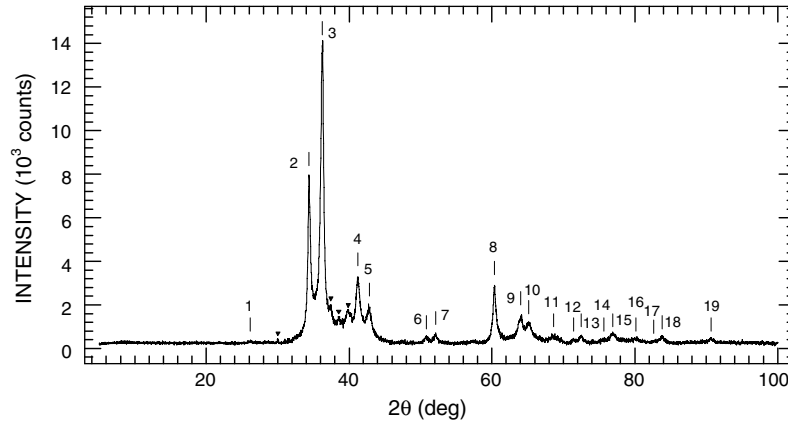
**Figure 1.** The XRD spectrum of an $Ag_{50}In_{36}Gd_{14}$ alloy at 298 K. The vertical lines labelled with integers above all detected i Bragg peaks correspond to the positions calculated for the Cu Kα_1 radiation, as explained in the text. The position, full width at half maximum, and relative intensity of each detected i peak are given in table 1 together with the corresponding index. The symbol ▼ indicates the peak positions corresponding to an unidentified second phase.

Table 1. Positions in terms of $2\theta_1$ (in deg) corresponding to Cu Kα_1 radiation and Q_{exp} (in Å^{-1}), full width at half maximum Γ_Q (in Å^{-1}), and relative intensity INT normalized to 100.0 of all detected icosahedral Bragg peaks, which are labelled with consecutive integers in column 1, as obtained from the fit [23]. The integers correspond to the vertical lines in figure 1. Q_{cal} (in Å^{-1}) is the calculated Q-value by taking the position of the second line with the $I1$ index 18/29 as the reference line. $I1$ and $I2$ are the indices (N/M) and $(h/h', k/k', l/l')$ based on the indexing scheme of Cahn *et al* [24], whereas $I3$ and $I4$ are the indices corresponding, respectively, to the indexing schemes of Elser [25] and Bancel *et al* [26].

Label	$2\theta_1$	Q_{exp}	Q_{cal}	Γ_Q	INT	$I1$	$I2$	$I3$	$I4$
1	26.146	1.845	1.842	0.025	0.5	12/16	022200	211000	$31\bar{1}\bar{1}\bar{1}1$
2	34.388	2.411	2.411	0.024	44.0	18/29	122300	211111	100000
3	36.229	2.536	2.535	0.027	100.0	20/32	002400	221001	110000
4	41.230	2.872	2.876	0.034	22.4	26/41	013400	222100	111101
5	42.832	2.978	2.980	0.037	11.3	28/44	222400	311111	210001
6	50.831	3.501	3.499	0.036	3.5	38/61	233400	322101	111000
7	52.104	3.582	3.585	0.039	4.4	40/64	242400	322111	111100
8	60.376	4.102	4.102	0.031	23.9	52/84	004600	332002	101000
9	64.008	4.323	4.321	0.040	13.3	58/93	233600	333101	210000
10	65.169	4.393	4.391	0.043	10.1	60/96	224600	422211	$210\bar{1}00$
11	68.637	4.599	4.596	0.069	6.9	66/105	104700	432002	$2111\bar{1}1$
12	71.426	4.761	4.758	0.034	1.7	70/113	124700	432112	110010
13	72.485	4.822	4.822	0.034	3.9	72/116	244600	433101	200000
14	75.698	5.005	5.009	0.052	2.7	78/125	344601	433201	211001
15	76.916	5.073	5.071	0.037	3.8	80/128	004800	442002	220000
16	80.149	5.251	5.249	0.085	3.5	86/137	364500	443101	310001
17	82.674	5.388	5.392	0.016	0.4	90/145	015800	522222	111110
18	83.815	5.448	5.448	0.041	4.1	92/148	115801	443102	211000
19	90.709	5.803	5.801	0.028	1.8	104/168	464600	533212	111010

to half-integer indices confirm that the i $Ag_{50}In_{36}Gd_{14}$ QC has a simple icosahedral (SI) six-dimensional Bravais lattice characteristic for i alloys that cannot be produced as
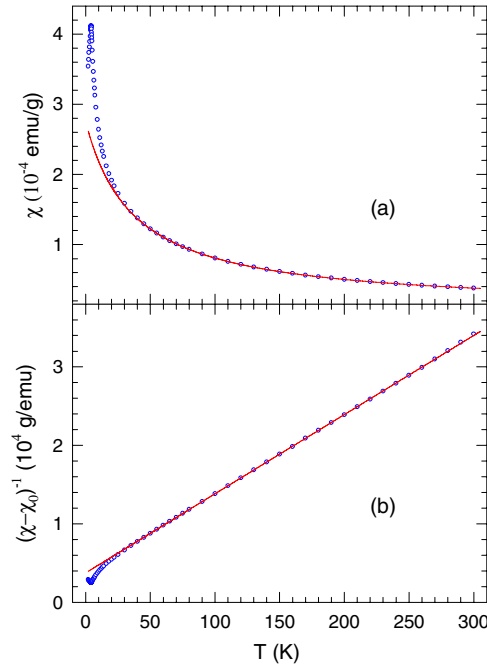
Figure 2. (a) The temperature dependence of the magnetic susceptibility of the icosahedral $Ag_{50}In_{36}Gd_{14}$, measured in an external magnetic field of 30 Oe. The solid line is the fit to equation (1) in the temperature range 50–300 K, as explained in the text. (b) The inverse magnetic susceptibility corrected for the contribution χ_0, $(\chi - \chi_0)^{-1}$ versus temperature T of the icosahedral $Ag_{50}In_{36}Gd_{14}$. The solid line is the fit to equation (1).

thermodynamically stable. The value of the six-dimensional hypercubic lattice constant calculated from the value Q_{exp} that corresponds to the (18, 29) i peak is 7.805(2) Å. The widths Γ_Q of the i peaks is significantly larger than the instrumental resolution (about $0.006\,\text{Å}^{-1}$) of the XRD spectrometer. This broadening, as well as the small shift of Q_{exp} from their ideal positions Q_{cal}, indicates the presence of some structural/chemical disorder in the i $Ag_{50}In_{36}Gd_{14}$ QC.

3.2. Magnetic susceptibility

The magnetic susceptibility χ of the i $Ag_{50}In_{36}Gd_{14}$ QC measured in an applied magnetic field of 30 Oe between 2.0 and 300 K is shown in figure 2(a). The sample was zero-field cooled to the lowest temperature and the measurement was performed while warming the sample up to 300 K. The $\chi(T)$ curve exhibits a definite peak at 4.20(5) K, indicating magnetic ordering. The $\chi(T)$ data above 50 K could be fitted to a modified Curie–Weiss law,

$$\chi = \chi_0 + \frac{C}{T - \theta_p}, \tag{1}$$

where χ_0 is the temperature-independent magnetic susceptibility, C is the Curie constant, and θ_p is the paramagnetic Curie temperature. The Curie constant can be expressed as $C = \frac{N\mu_{eff}^2}{3k}$, where N is the concentration of magnetic atoms per unit mass and μ_{eff} is the effective magnetic moment. Figure 2(b) shows the inverse magnetic susceptibility corrected for the contribution χ_0, $(\chi - \chi_0)^{-1}$ versus temperature; the validity of the Curie–Weiss law is evident. The values
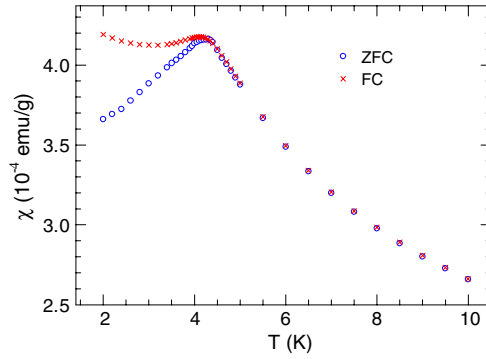
Figure 3. The temperature dependence of the zero-field-cooled (ZFC) and field-cooled (FC) magnetic susceptibility of the icosahedral $Ag_{50}In_{36}Gd_{14}$, measured in an external magnetic field of 30 Oe.

of χ_0, C, and θ_p obtained from the fit are, respectively, $8.57(10) \times 10^{-6}$ emu g^{-1}, $9.91(3) \times 10^{-3}$ emu K g^{-1}, and $-37.1(2)$ K. This value of C corresponds to μ_{eff} of $8.15(1)$ μ_B per Gd atom.

For a free Gd^{3+} ion (electronic ground state $^8S_{7/2}$), the theoretical value of $\mu_{eff}^{th} = g\mu_B\sqrt{J(J+1)}$ is 7.94 μ_B [27]. The fact that the experimental value $\mu_{eff} = 8.15(1)$ μ_B is very close to the theoretical value of 7.94 μ_B confirms that the magnetic moment is localized on the Gd^{3+} ions and that, as expected, Ag and In atoms carry no magnetic moment. The negative value of θ_p indicates the predominantly antiferromagnetic interaction between the Gd^{3+} spins.

To determine the nature of the magnetic transition at 4.20 K, we measured the temperature dependence of the zero-field-cooled (ZFC) and field-cooled (FC) magnetic susceptibility around 4.2 K in an applied magnetic field of 30 Oe (figure 3). The occurrence of a bifurcation between the ZFC and FC data at the freezing temperature $T_f = 4.25(5)$ K is evident. Above T_f both ZFC and FC data are identical. Such a behaviour of the ZFC and FC susceptibility data is characteristic of a spin glass [28]. The i $Ag_{50}In_{36}Gd_{14}$ QC is thus a spin glass with a freezing temperature $T_f = 4.25(5)$ K.

The occurrence of a spin-glass behaviour requires both randomness and frustration [28, 29]. The frustration parameter f, defined as $f = -\theta_p/T_f$ [30], is an empirical measure of frustration. Its value for the i $Ag_{50}In_{36}Gd_{14}$ QC is $8.7(1)$, which indicates that the studied QC belongs to a category of strongly geometrically frustrated magnets [30].

There are two other Gd-containing i alloys, $Zn_{50}Mg_{42}Gd_8$ with face-centred icosahedral (FCI) structure [31] and $Cd_{50}Mg_{40}Gd_{10}$ with SI structure [32], which are also spin glasses. The values of θ_p and T_f for these i alloys are, respectively, -38 K, 5.5 K and $-37.8(1.0)$ K, 4.3(1) K. These are very similar to the values of $-37.1(2)$ K, 4.25(5) K found here for the i $Ag_{50}In_{36}Gd_{14}$ QC with SI structure. It would thus appear that SI and FCI Gd-containing i alloys have very similar bulk magnetic properties.

All three known Gd-containing ternary i alloys, $Zn_{50}Mg_{42}Gd_8$ [31], $Cd_{50}Mg_{40}Gd_{10}$ [32], and $Ag_{50}In_{36}Gd_{14}$ studied here, exhibit no long-range magnetic order and are spin glasses. Is then the spin-glass state inherent to the quasicrystalline structure of these alloys or does it result from structural/chemical disorder present in them? $Zn_{50}Mg_{42}Gd_8$ and $Cd_{50}Mg_{40}Gd_{10}$ QCs are thermodynamically stable, whereas the $Ag_{50}In_{36}Gd_{14}$ QC is metastable. The fact that the spin-glass state occurs both in thermodynamically stable and metastable i QCs seems to exclude the structural disorder as the main reason for its occurrence. These three Gd-containing ternary i QCs possess some chemical disorder which may lead to the development of the
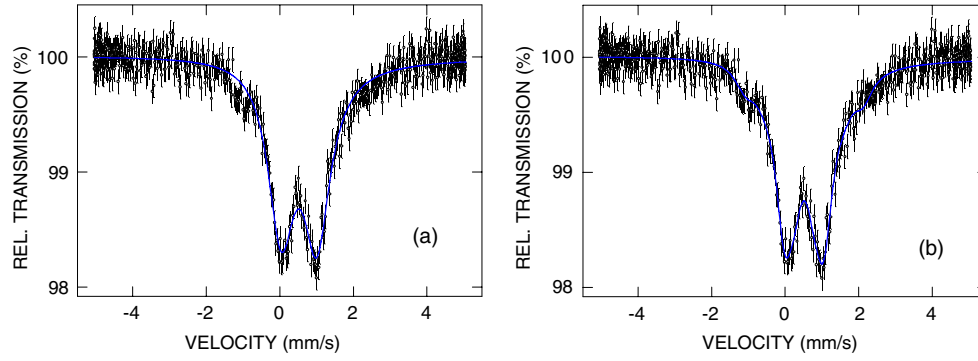
Figure 4. The ^{155}Gd Mössbauer spectrum of the icosahedral Ag$_{50}$In$_{36}$Gd$_{14}$ at 10.4 K fitted (solid line) with (a) one quadrupole pattern and (b) a distribution of quadrupole patterns. The zero-velocity scale is relative to the source.

spin-glass state. The fact that the thermodynamically stable binary i QC YbCd$_{5.7}$ with no chemical disorder is not a spin glass [33] seems to support this suggestion.

3.3. Mössbauer spectroscopy

Figure 4(a) shows a ^{151}Gd Mössbauer spectrum of the i Ag$_{50}$In$_{36}$Gd$_{14}$ QC at 10.4 K, i.e., well above $T_{\rm f}$. This spectrum exhibits a substantial electric quadrupole hyperfine interaction. For ^{155}Gd nuclei, the quadrupole moment of the excited nuclear state with spin $I_{\rm ex} = 5/2$, $Q_{\rm ex} = 0.12$ b [19], is significantly smaller than that of the ground nuclear state with spin $I_g = 3/2$, $Q_g = 1.30$ b [34]. This causes the quadrupole splitting of the excited nuclear state, which is sensitive to the sign of V_{zz} and the magnitude of η, to be smaller than the natural linewidth $\Gamma_{\rm nat} = 0.250$ mm s^{-1}. Consequently, only the absolute value of the effective quadrupole splitting parameter $\Delta_g^{\rm eff} = eQ_g|V_{zz}|\sqrt{1 + \eta^2/3}$ can be derived from a Mössbauer spectrum of a sample in the paramagnetic state [35]. The parameters derived from the fit ($\chi^2 = 1.10$) of the 10.6 K Mössbauer spectrum (figure 4(a)) are: the isomer shift (relative to the ^{155}Eu(SmPd$_3$) source) $\delta = 0.513(8)$ mm s^{-1}, $\Delta_g^{\rm eff} = 2.030(27)$ mm s^{-1}, $f_{\rm a} = 9.9(2)\%$, and $\Gamma_{\rm a} = 0.508(23)$ mm s^{-1}. Although a relatively good fit was obtained, the value of $\Gamma_{\rm a}$ is unphysically large. This large value of $\Gamma_{\rm a}$ indicates the presence of a distribution of $\Delta_g^{\rm eff}$. In a QC, variations of the local coordination from site to site are expected to give rise to a distribution of the parameters V_{zz} and η [36]. The distribution of $\Delta_g^{\rm eff}$ was simulated by fitting the 10.6 K Mössbauer spectrum with six component quadrupole patterns with $\Delta_g^{\rm eff}$-values extending from 0.0 to 1.5 mm s^{-1}; the absorber linewidth was fixed to the value of $\Gamma_{\rm nat}$ and the same values of δ and $f_{\rm a}$ were assumed for all components. The parameters deduced from the fit assuming a distribution of $\Delta_g^{\rm eff}$ (figure 4(b)), δ, the average $\Delta_g^{\rm eff}$, $\bar{\Delta}_g^{\rm eff}$, and $f_{\rm a}$ are given in table 2. The ^{151}Gd Mössbauer spectra of the i Ag$_{50}$In$_{36}$Gd$_{14}$ QC at 5.9 and 5.3 K (figure 5) display the presence of a distribution of $\Delta_g^{\rm eff}$ and were fitted in the same way as the corresponding spectrum of the i Ag$_{50}$In$_{36}$Gd$_{14}$ QC at 10.6 K; the parameters derived from the fits are given in table 2.

The ^{151}Gd Mössbauer spectrum of the i Ag$_{50}$In$_{36}$Gd$_{14}$ QC at 4.4 K, i.e., slightly above $T_{\rm f}$, clearly shows (figure 5) the presence of a combined electric quadrupole and magnetic dipole hyperfine interactions. It was analysed by assuming a distribution of the quadrupole splitting constant $\Delta_g = eQ_gV_{zz}$, and the same value of $H_{\rm hf}$ was used for all component patterns; the value of θ was fixed to 0.0° in the fit. The negative value of the average Δ_g, $\bar{\Delta}_g = eQ_g\bar{V}_{zz}$, obtained from the fit (table 2) clearly establishes that the V_{zz} component of the
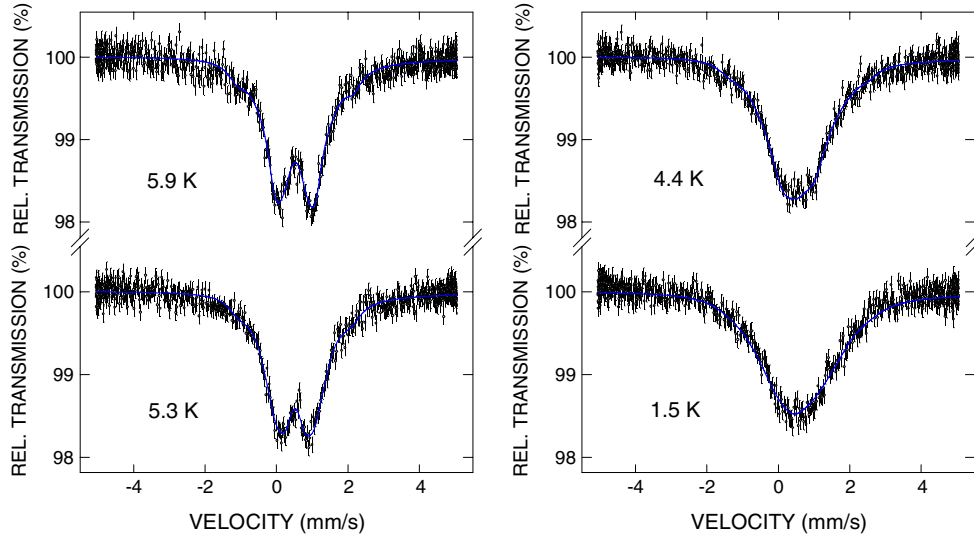
Figure 5. ^{155}Gd Mössbauer spectra of the icosahedral $Ag_{50}In_{36}Gd_{14}$ at various temperatures. Solid lines are fits, as described in the text. The zero-velocity scale is relative to the source.

Table 2. Hyperfine interaction parameters derived from the fits to the ^{151}Gd Mössbauer spectra of the icosahedral $Ag_{50}In_{36}Gd_{14}$ at various temperatures.

T (K)	δ (mm s^{-1})	$\bar{\Delta}_g^{\mathrm{eff}}$ or $\bar{\Delta}_g$ (mm s^{-1})	η	H_{hf} (kOe)	f_a (%)	χ^2
10.4	0.511(7)	2.498(37)			9.9(1)	0.99
5.9	0.522(7)	2.541(51)			10.0(1)	1.06
5.3	0.512(8)	2.385(87)			10.0(1)	1.19
4.4	0.501(9)	−2.212(45)	1.00(20)	69.8(7.5)	10.1(2)	1.04
1.5	0.516(16)	−2.426(95)	0.84(24)	119.6(11.2)	10.5(2)	1.10

EFG tensor at the Gd sites in the i $Ag_{50}In_{36}Gd_{14}$ QC is negative. The complete set of the EFG tensor parameters at the Gd sites in the i $Ag_{50}In_{36}Gd_{14}$ QC determined experimentally here is: $\bar{V}_{zz} = -4.91(10) \times 10^{21}$ V cm^{-2} and $\eta = 1.00(20)$. The ^{151}Gd Mössbauer spectrum of the i $Ag_{50}In_{36}Gd_{14}$ QC at 1.5 K (figure 5) was fitted in the same way as the corresponding spectrum at 4.4 K; the parameters derived from the fit are given in table 2.

The studied i $Ag_{50}In_{36}Gd_{14}$ QC is formed [12] by replacing all of Cd in the binary i $YbCd_{5.7}$ QC [13] with Ag and In, and Yb with Gd. It is thus expected that the crystal structure of the i $Ag_{50}In_{36}Gd_{14}$ QC must be similar to that of the i $YbCd_{5.7}$ QC. The crystal structure of the i $YbCd_{5.7}$ QC has been recently solved [14]. One would expect that Gd atoms are located at the Yb sites (on the vertices of the icosahedron and inside the acute rhombohedron) and that the Ag and In atoms are distributed among the Cd sites. Clearly, the existence of the multiplicity of Gd sites observed here is compatible with this structural model. The complete set of the EFG tensor parameters at the Gd sites in the i $Ag_{50}In_{36}Gd_{14}$ QC determined experimentally here could be compared with the corresponding parameters obtained from *ab initio* calculations of the EFGs for a possible structural model for the i $Ag_{50}In_{36}Gd_{14}$ QC, similarly as has been done for the i Al–Cu–Fe QC [37]. This could lead to the solution of the structure of the i $Ag_{50}In_{36}Gd_{14}$ QC.

In terms of the Debye approximation of the lattice vibrations, the absorber Debye–Waller factor f_a is expressed [18] by the Debye temperature, Θ_D, as

$$f_a(T) = \exp\left\{-\frac{3}{4}\frac{E_\gamma^2}{Mc^2 k\Theta_D}\left[1+\left(\frac{T}{\Theta_D}\right)^2\int_0^{\Theta_D/T}\frac{x\,\mathrm{d}x}{\mathrm{e}^x-1}\right]\right\}, \tag{2}$$

where E_γ is the energy of the Mössbauer transition, M is the mass of the Mössbauer nucleus, c is the speed of light, and k is the Boltzmann constant. The analysis of the values of f_a given in table 2 via equation (2) yields $\Theta_D = 199(2)$ K. This is the lowest value among the known ternary i QCs. This value compares well with the anomalously low value of Θ_D (in the range 138–145 K) for the i $Yb_{5.7}Cd$ QC [33, 38].

The freezing temperature determined by the Mössbauer effect, T_f^m, is defined as a temperature at which the magnetic dipole hyperfine interaction sets in. The presence of the magnetic dipole hyperfine interaction in the Mössbauer spectrum of the i $Ag_{50}In_{36}Gd_{14}$ QC at 4.4 K, and its absence in the Mössbauer spectrum at 5.3 K, shows that T_f^m lies between 4.4 and 5.3 K. Clearly, T_f^m is larger than T_f. The systematically higher values of T_f^m than T_f have been observed for many spin-glass systems [28, 39]. The inequality $T_f^m > T_f$ results from a time window of an experimental technique used to determine the freezing temperature: as the time window decreases, the freezing temperature increases [28, 39].

4. Conclusions

A newly discovered icosahedral quasicrystal $Ag_{50}In_{36}Gd_{14}$ has been studied with x-ray diffraction, magnetic susceptibility, and ^{155}Gd Mössbauer spectroscopy. The studied quasicrystal has a simple six-dimensional Bravais lattice with the six-dimensional hypercubic lattice constant of 7.805(2) Å. The observed broadening of the diffraction Bragg peaks reflects the presence of the topological/chemical disorder. The temperature dependence of the magnetic susceptibility follows the Curie–Weiss law with the effective magnetic moment of 8.15(1) μ_B per Gd atom and the paramagnetic Curie temperature of $-37.1(2)$ K. The studied quasicrystal is a spin glass with a freezing temperature of 4.25(5) K. The presence of the distribution of the electric quadrupole splitting in the Mössbauer spectra indicates the existence of a multiplicity of Gd sites. The values of the principal component of the electric field gradient tensor and the asymmetry parameter at these sites are, respectively, $-4.91(10) \times 10^{21}$ V cm^{-2} and $\eta = 1.00(20)$. The Debye temperature of the studied quasicrystal is 199(2) K. The hyperfine magnetic field sets in at a temperature higher than the freezing temperature.

Acknowledgments

References

[1] Shechtman D, Blech I, Gratis D and Cahn J W 1984 *Phys. Rev. Lett.* **53** 1951
[2] Suck J-B, Schreiber M and Häussler P (ed) 2002 *Quasicrystals, an Introduction to Structure, Physical Properties, and Applications* (Berlin: Springer)
[3] Lifshitz R 1995 *Proc. 5th Int. Conf. Quasicrystals* ed C Janot and E Mosseri (Singapore: World Scientific) p 43
    Lifshitz R 1998 *Phys. Rev. Lett.* **80** 2717
    Lifshitz R 2000 *Mater. Sci. Eng.* A **294–296** 508
    Lifshitz R and Mandel S E-D 2004 *Acta Crystallogr.* A **60** 167
[4] Godrèche C, Luck J M and Orland H 1986 *J. Stat. Phys.* **45** 777
    Bhattacharjee S M, Ho J-S and Johnson J A Y 1987 *J. Phys. A: Math. Gen.* **20** 4439

　　　Okabe Y and Niizeki K 1988 *J. Phys. Soc. Japan* **57** 16
　　　Duneau M, Dunlop F, Jagannathan A and Oguey C 1991 *Mod. Phys.* B **5** 1895
　　　Matsuo S, Ishimasa T and Nakano H 2000 *Mater. Sci. Eng.* A **294–296** 633
　　　Matsuo S, Ishimasa T and Nakano H 2002 *J. Magn. Magn. Mater.* **246** 223
　　　Matsuo S, Nakano H, Motomura S and Ishimasa T 2005 *J. Phys. Soc. Japan* **74** 1036
　　　Matsuo S, Motomura S and Ishimasa T 2007 *Phil. Mag.* **87** 51
 [5]　Ledue D, Teillet J, Carnet J and Dujardin J 1993 *J. Non-Cryst. Solids* **153/154** 403
　　　Reid R W, Bose K and Mitrovi B 1998 *J. Phys.: Condens. Matter* **10** 2303
　　　Hermission J 2000 *J. Phys. A: Math. Gen.* **33** 57
 [6]　Wessel S, Jagannathan A and Hass S 2003 *Phys. Rev. Lett.* **90** 177205
　　　Vedmedenko E Y, Oepen H P and Kirschner J 2003 *Phys. Rev. Lett.* **90** 137203
　　　Jagannathan A 2004 *Phys. Rev. Lett.* **92** 047202
　　　Vedmedenko E Y, Grimm U and Wiesendanger R 2004 *Phys. Rev. Lett.* **93** 076407
　　　Jagannathan A 2005 *Phys. Rev.* B **71** 115101
　　　Vedmedenko E Y 2004 *Ferroelectrics* **305** 129
　　　Vedmedenko E Y, Grimm U and Wiesendanger R 2006 *Phil. Mag.* **86** 733
 [7]　Jagannathan A and Schultz H J 1997 *Phys. Rev.* B **55** 8045
　　　Hida K 2001 *Phys. Rev. Lett.* **86** 1331
 [8]　Stadnik Z M, Stroink G, Ma H and Williams G 1989 *Phys. Rev.* B **39** 9797
　　　Fukamichi K 1999 *Physical Properties of Quasicrystals* ed Z M Stadnik (Berlin: Springer) p 295
 [9]　Charrier B, Ouladdiaf B and Schmitt D 1997 *Phys. Rev. Lett.* **78** 4637
[10]　Sato T J, Takakura H, Tsai A P and Shibata K 1998 *Phys. Rev. Lett.* **81** 2364
　　　Noakes D R, Kalvius G M, Wäppling R, Stronach C E, White M F Jr, Saito H and Fukamichi K 1998 *Phys. Lett.*
　　　　A **238** 197
　　　Islam Z, Fisher I R, Zarestky J, Canfield P C, Stassis C and Goldman A I 1998 *Phys. Rev.* B **57** R11047
[11]　Sato T J, Takakura H, Tsai A P, Shibata K, Ohoyama K and Andersen K H 2000 *Phys. Rev.* B **61** 476
　　　Sato T J, Takakura H, Tsai A P, Ohoyama K, Shibata K and Andersen K H 2000 *Mater. Sci. Eng.* A **294–296** 481
　　　Sato T J, Takakura H, Guo J, Tsai A P and Ohoyama K 2002 *J. Alloys Compounds* **342** 365
　　　Sato T J 2005 *Acta Crystallogr.* A **61** 39
　　　Sato T J, Takakura H, Tsai A P and Shibata K 2006 *Phys. Rev.* B **73** 054417
[12]　Iwano S, Nishimoto H, Tamura R and Takeuchi S 2006 *Phil. Mag.* **86** 435
[13]　Tsai A P, Guo J Q, Abe E, Takakura H and Sato T J 2000 *Nature* **408** 537
　　　Guo J Q, Abe E and Tsai A P 2000 *Phys. Rev.* B **62** R14605
[14]　Takakura H, Gómez C P, Yamamoto A, de Boissieu M and Tsai A P 2007 *Nat. Mater.* **6** 58
[15]　Wong-Ng W and Hubbard C R 1987 *Powder Diffr.* **2** 242
[16]　*Standard Reference Material 640c, Silicon Powder Line Position and Line Shape Standard for X-ray Diffraction*
　　　　2000 (US: Natl. Inst. Stand. Techn)
[17]　Otterloo B F, Stadnik Z M and Swolfs A E M 1983 *Rev. Sci. Instrum.* **54** 1575
[18]　Greenwood N N and Gibb T C 1971 *Mössbauer Spectroscopy* (London: Chapman and Hall)
　　　Gütlich P, Link R and Trautwein A 1978 *Mössbauer Spectroscopy and Transition Metal Chemistry* (Berlin:
　　　　Springer)
[19]　Armon H, Bauminger E R and Ofer S 1973 *Phys. Lett.* B **43** 380
[20]　Stadnik Z M and Żukrowski J 2005 unpublished results
[21]　Margulies S and Ehrman J R 1961 *Nucl. Instrum. Methods* **12** 131
　　　Shenoy G K, Friedt J M, Maletta H and Ruby S L 1974 *Mössbauer Effect Methodology* vol 10, ed I J Gruverman,
　　　　C W Seidel and D K Dieterly (New York: Plenum) p 277
[22]　Jenkins R and Schreiner W N 1989 *Powder Diffr.* **4** 74
[23]　Schreiner W N and Jenkins R 1983 *Adv. X-ray Anal.* **26** 141
[24]　Cahn J W, Shechtman D and Gratias D 1986 *J. Mater. Res.* **1** 13
[25]　Elser V 1986 *Acta Crystallogr.* A **42** 36
[26]　Bancel P A, Heiney P A, Stephens P W, Goldman A I and Horn P M 1985 *Phys. Rev. Lett.* **54** 2422
[27]　Ashcroft N W and Mermin N D 1976 *Solid State Physics* (Philadelphia, PA: Saunders)
[28]　Mydosh J A 1993 *Spin Glasses: an Experimental Introduction* (London: Taylor and Francis)
[29]　Toulouse G 1977 *Commun. Phys.* **2** 116
　　　Binder K and Young A P 1986 *Rev. Mod. Phys.* **58** 801
[30]　Ramirez A P 2001 *Handbook of Magnetic Materials* vol 13, ed K H J Buschow (Amsterdam: Elsevier) p 423
[31]　Hattori Y, Niikura A, Tsai A P, Inoue A, Masumoto T, Fukamichi K, Aruga-Katori H and Goto T 1995 *J. Phys.:*
　　　　Condens. Matter **7** 2313

[32] Sebastian S E, Huie T, Fisher I R, Dennis K W and Kramer M J 2004 *Phil. Mag.* **84** 1029

[33] Dhar S K, Palenzona A, Manfrinetti P and Pattalwar S M 2002 *J. Phys.: Condens. Matter* **14** 517

[34] Tanaka Y, Laubacher D B, Steffen R M, Shera E B, Wohlfahrt H D and Hoehn M V 1982 *Phys. Lett.* B **108** 8

[35] Czjzek G 1993 *Mössbauer Spectroscopy Applied to Magnetism and Materials Science* vol 1, ed G J Long and F Grandjean (New York: Plenum) p 373

[36] Stadnik Z M 1996 *Mössbauer Spectroscopy Applied to Magnetism and Materials Science* vol 2, ed G J Long and F Grandjean (New York: Plenum) p 125

[37] Zijlstra E S, Kortus J, Krajčí M, Stadnik Z M and Bose S K 2004 *Phys. Rev.* B **69** 094206

[38] Tamura R, Murao Y, Takeuchi S, Tokiwa K, Watanabe T, Sato T J and Tsai A P 2001 *Japan. J. Appl. Phys.* **40** L912

Pope A L, Tritt T M, Gagnon R and Strom-Olsen J 2001 *Appl. Phys. Lett.* **79** 2345

Tamura R, Murao Y, Kishino S, Takeuchi S, Tokiwa K and Watanabe T 2004 *J. Mater. Sci. Eng.* A **375–377** 1002

Kramer M J, Lograsso T A and Sordelet D J 2005 *Phil. Mag. Lett.* **85** 151

[39] Murani A P 1977 *J. Magn. Magn. Mater.* **5** 95

Murani A P 1981 *J. Magn. Magn. Mater.* **22** 271

Wagner H G and Gonser U 1983 *J. Magn. Magn. Mater.* **31–34** 1343

Meyer C, Hartmann-Boutron F, Gros Y and Campbell I A 1985 *J. Magn. Magn. Mater.* **46** 254

Aruga H, Tokoro T and Ito A 1988 *J. Phys. Soc. Japan* **57** 261

Bogner J, Reissner M, Steiner W and Dubiel S M 1998 *J. Phys.: Condens. Matter* **10** 9849